# A cable-driven exoskeleton to control ankle mobility during gait in children with cerebral palsy

Iñaki Dellibarda Varela
*ETSI Telecomunicación*
*Universidad Politécnica de Madrid (UPM)*
Madrid, Spain
i.dellibarda@alumnos.upm.es

Pablo Romero-Sorozabal
*Centro de Automática y Robótica*
*Consejo Superior de Investigaciones Científicas (CSIC-UPM)*
Madrid, Spain
pablo.romero@csic.es

Gabriel Delgado-Oleas
*Centro de Automática y Robótica*
*Consejo Superior de Investigaciones Científicas (CSIC-UPM)*
Madrid, Spain
Ingeniería Electrónica, Universidad del Azuay
gabriel.delgado@csic.es

Álvaro Gutiérrez
*ETSI Telecomunicación*
*Universidad Politécnica de Madrid (UPM)*
Madrid, Spain
a.gutierrez@upm.es

Jorge Muñoz
*Centro de Automática y Robótica*
*Consejo Superior de Investigaciones Científicas (CSIC-UPM)*
Madrid, Spain
jorge.munoz@csic.es

Eduardo Rocon
*Centro de Automática y Robótica*
*Consejo Superior de Investigaciones Científicas (CSIC)*
Madrid, Spain
e.rocon@csic.es

2024 7th Iberian Robotics Conference (ROBOT) | 979-8-3503-7636-4/24/$31.00 ©2024 IEEE | DOI: 10.1109/ROBOT61475.2024.10796916

***Abstract*—Cerebral palsy is the most common neurological disorder in children. In the search for effective treatments, robot-assisted therapy techniques have emerged in recent years, combining physiotherapy with the use of exoskeletons for rehabilitation. In this context, the Discover2Walk project was developed, a cable-driven modular exoskeleton designed for early gait rehabilitation. In this paper, a novel method for foot and ankle joint control, easily implementable in the Discover2Walk, is presented. This method is capable of directing movement in three degrees of freedom: two translational (cartesian x and z axes) and one rotational (dorsiflexion and plantar flexion). The results obtained demonstrate the viability of the proposed system in controlling motion in the three degrees of freedom of interest.**

***Index Terms*—modular exoskeleton, cable actuation, cerebral palsy, impedance control, robot-assisted therapy.**

## I. Introduction

Cerebral Palsy (CP) is a disorder originating in the Central Nervous System (CNS) which affects 2 to 2.5 out of every 1000 babies born, being the most common neurological disorder in children [1]. It is characterized by a progressive loss of sensory and motor capacity and the Symptoms associated with CP include the prevalence of pain and movement and gait disorders. Loss of walking ability has been shown to be associated with significant impairment of health and quality of life [2].

This research was funded by the Spanish Ministry of Science and Innovation, project Discover2Walk (PID2019-105110RB-C31). PRZ received a Training Program fellowship (PRE2020-092049) from the Ministry of Science and Innovation.

To reduce these problems, the most common treatment is physiotherapy, due to the positive results obtained [2]. In recent years, the use of exoskeletons as a therapy for CP has become widespread. This approach complements treatments such as physiotherapy or surgery, which often struggle to maintain patients' muscle strength over time [3]. These techniques also facilitate passive movement in children and allow them to experience greater freedom of movement.

The robotic devices base their therapies on the repetitive and intensive performance of specific training tasks, with the aim of improving neuroplasticity, motor skills and muscle strength in children with CP [4]. This type of treatment is known as *robot-assisted therapy* [5], [6]. Some well-known examples of exoskeletons for gait rehabilitation or assistance are: Lokomat [7], Innowalk [8] and CPWalker (developed by our research group) [9].

This article focuses on the Discover2Walk (D2W) exoskeleton (Fig. 1), a pediatric modular platform designed for gait rehabilitation. The system utilizes cable-driven actuators to guide the movement of children in the early stages of CP, facilitating walking and exploration of their environment at an age comparable to that of healthy children [10]. It is an end-effector type device where the robot connects to the patient's joints via lightweight cables at distal points. The forces generated at these distal interfaces are transmitted to produce movements in the patient's joints [11].

Within the D2W exoskeleton modules, our focus is on the ankle control module, featuring a novel system with 4

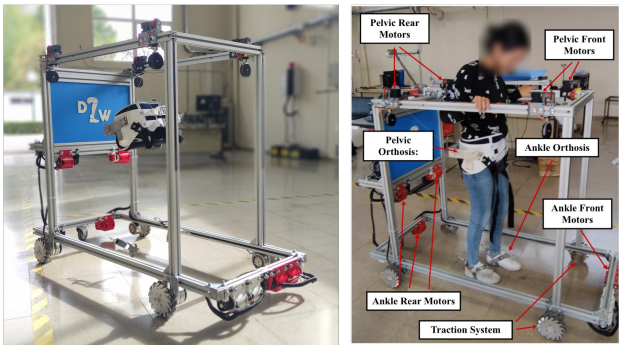


Fig. 1: D2W exoskeleton consisting of pelvis control module, ankle and traction system.

brushless motors mounted on dual coil drums, each with two associated cables. This configuration enables control of three degrees of freedom (DOF): two translational (Cartesian $x$ and $z$ axes) and one rotational (dorsiflexion and plantar flexion, denoted as $pitch$ in Euler's angles notation). Unlike the original D2W ankles' system, which only controlled translational movements. This improvement responds to feedback from clinicians associated with the project, who emphasize the importance of rotational control. In this article, we will describe the development, implementation and testing of the new ankles' system.

## II. Discover2Walk structure

The D2W (Fig. 1) has a flexible structure that easily adapts to the patient's characteristics and is focused on treating children between the ages of two and five. Unlike rigid exoskeletons, by controlling the movement of children through cables, this extra component of flexibility is acquired, increasing the child's ability to explore his environment and motor skills [12].

### A. Pelvic Module

Consists of four Dynamixel XH540-W150-T servomotors (ROBOTIS, United States) anchored to the upper vertices of the D2W frame. Each motor is associated with a Kevlar cable, which also connects to a commercial pelvic orthosis (PRIM, Spain) fitted to the patient.

To monitor the pelvis and control the partial body weight support it provides, this module has three main types of sensors: inertial measurement units (IMUs), motor absolute encoders and load cells. These sensors measure the cables' length, the pelvis's orientation and the weight supported by each cable.

The described structure and configuration of motors and sensors allow the three-dimensional control of the pelvis in six DOF, three translational and three rotational.

### B. Ankle Module

The current ankle control system consists of six brushless motor, model DUAL SHAFT MOTOR-D6374 150KV (OdriveRobotics, United States), three motors per ankle. Each motor is associated with encoder AMT102-V type sensors (CUIDevices, USA) to measure length, and a Kevlar cable which is anchored to the ankles using modified commercial foot straps (SYL Fitness®).

The current ankle module allows control of motion in the longitudinal and vertical direction of motion (two translational DOF). It does not have the capacity of controlling dorsiflexion and plantar flexion rotations. Given the importance of being able to control this rotation for a correct gait cycle, a new system developed for ankle control will be explained in this article.

### C. Traction Module

It allows the translation and rotation of the entire platform, facilitating the movement of the infant. For this purpose, it has four aluminum wheels with a diameter of 254 mm and a capacity of 40 kg each (Nexus Robot, China). To assist the movement, each wheel is powered by an EC 90 Flat 600W brushless motor (MAXON, Switzerland).

Additionally, to determine the orientation of the platform, a BNO055 IMU sensor (BoschSensortec, Germany) is placed at the front. Each motor is also equipped with an AMT102-V encoder to measure the position and speed of the wheels.

### D. System Architecture

The D2W is based on a bio-inspired control structure that mimics the CNS. This hierarchical structure is divided into three levels: high, medium and low, Fig. 2.

The *high level* is the one associated with perception and intention. It is implemented through a clinical interface in which the patient's height and weight and key parameters associated with gait are established. It is also responsible for giving the initial movement command.

The *middle level* is in charge of generating the target gait patterns to be reached by the subject. These trajectories are established according to the patient's parameters, as well as by the three-dimensional estimation of the joint centers and their speed of movement in real-time, and are used as setpoints to synchronize the action of the low level.

The *low level* is responsible for each of the actuators (pelvis, ankle and traction module) to reach the setpoints established

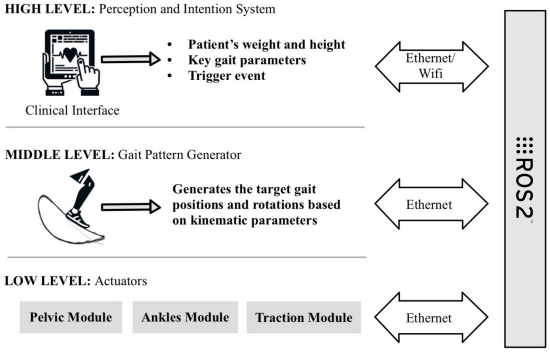


Fig. 2: D2W bio-inspired architecture based on three hierarchical levels.

by the medium level. As in the human body, each actuator has sensors to measure the current gait characteristics.

This architecture has been implemented through a system of publisher-subscriber nodes in ROS2, allowing modularity and communication between the different levels.

## III. Ankle Actuation System

This section discusses in detail the ankles' system module capable of controllin three DOFs of interest (translations $x$ and $z$ and rotation $pitch$). For this purpose, it is reviewed its mechanics, electronics, kinematic models and control system.

### A. Mechanical System

The new module is configured as a Cable-Driven Parallel Robot (CDPR) of type 1R2T, meaning it controls three DOF: two translational and one rotational. Such robots adhere to the relation $m + 1 = n$, where $m$ is the number of DOFs and $n$ is the number of cables [13]. Consequently, the system requires four cables arranged in the sagittal plane and placed in a rectangular prism shaped frame structure made of aluminum profiles (BoschSensortec, Germany), with dimensions 102x58x68 cm (Fig. 3). Covering the step lenth for children between six and twelve years of age (45 and 60 cm) [16].

In addition, to treat uncontrolled abduction-adduction rotations of the ankle and improve lateral ankles stabilization, each motor is mounted on a drum with a double coil that simultaneously controls two cables per motors, see Fig. 4). This design results in four redundant cables configuration, limiting the motion on the lateral plane without the need of including more actuators on the desing. Therefore, each ankle will be controlled by eight cables.

The specific drum configuration is shown in Fig. 4 a). It is a system of housings that cover the mechanical elements of the structure (motor, drums, and bearings), as well as a central axis 18 cm long that allows the simultaneous movement of the two drums. The structure is anchored to the BOSCH profiles by connecting arms. All parts were printed in PLA, except for the central axis, which is printed in PET as it requires greater strength.

The motion transition to patient is obtained through a developed ankle orthosis sole attached to the patient's foot, see Fig. 3. It presents four anchor points for the cables, allowing the correct fastening and control over the ankle. The insole was printed in PET to ensure its strength.

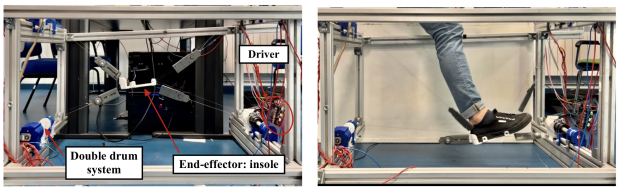


Fig. 3: Final structure of the test bench, with the mechanical and electronic components implemented.

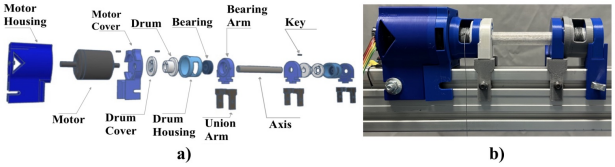


Fig. 4: a) Schematic of disassembled mechanical structure; b) Image of the final mechanical structure.

### B. Electronic System

The system is controlled by a computer running a Linux-based operating system, which communicates via USB serial with two motor drivers, Odrive V3.6 drivers (Odrive Robotics, United States). Both motor drivers are powered by a 48V HRPG-450-48 (Mean Well Enterprises Co., Taiwan) and each of them controls a pair of brushless motors, DUAL SHAFT MOTOR - D374 150 KV (Odrive Robotics, United States) and read their respective AMT10 encoders (Fig. 3).

### C. Kinematic Model

For controlling a system it is first needed a model of it, here it is presented the kinematic model of the system.

*1) Inverse Kinematics:* ($\boldsymbol{\varphi}^{\mathbf{IK}}$): allows to obtain the target lengths of the cables ($\vec{l} = [\vec{l_1}, ..., \vec{l_n}]$), to reach the target position in space and is defined by:

$$\boldsymbol{\varphi}^{\mathbf{IK}}(\vec{r}, \mathbf{R}) = \vec{l} \tag{1}$$

$$l_i = \| \vec{l_i} \| = \| \vec{a_i} - \vec{r} - \mathbf{R}\vec{b_i} \| \tag{2}$$

$$\mathbf{R} = \mathbf{R_x}(roll) \cdot \mathbf{R_y}(pitch) \cdot \mathbf{R_z}(yaw) \tag{3}$$

$$\vec{r} = (x, y, z) \tag{4}$$

where $\vec{r}$ ($\vec{r} \in \mathbb{R}^3$) is the cartesian setpoint position of the end-effector center with respect to the exoskeleton absolute coordinate system; $\mathbf{R}$ ($\mathbf{R} \in \mathbb{R}^{3x3}$) is the rotation matrix of the end-effector, dependent on the *roll*, *pitch* and *yaw* target angles (Euler angles notation); $l_i$ is the length of the $i^{th}$ cable; $\vec{a_i}$ ($\vec{a_i} \in \mathbb{R}^3$) is the position of the $i^{th}$ drum with respect to the exoskeleton coordinate system; $\vec{b_i}$ ($\vec{b_i} \in \mathbb{R}^3$) is the position of the end-effector anchors with respect to the end-effector moving reference system (Fig. 5).

*2) Forward Kinematics:* The calculation by forward kinematics ($\boldsymbol{\varphi}^{\mathbf{FK}}$) allows obtaining the position of the center of the end-effector and its rotation from the lengths of the cables and the dimensions of the reference frame.

The computation of the $\boldsymbol{\varphi}^{\mathbf{FK}}$ involves a non-trivial process since the position of the end-effector is defined as the intersection of the spheres of radius $l_i$ and centered at $A_i$, resulting in a overdetenmined system, [13]. To solve this problem, a numerical approach based on nonlinear least squares fitting is proposed:

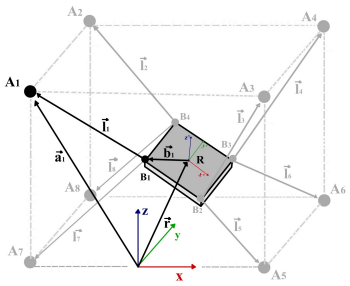

Fig. 5: Geometric schematic of the ankle module, in which $A_i$, $\vec{a_i}$, $B_i$, $\vec{b_i}$ represent the anchor points and vectors of the anchor points distal to the end-effector; $\vec{l_i}$ represents the cable vector; $\vec{r}$ is the Cartesian position of the end-effector and $\mathbf{R}$ the rotation matrix.

$$\psi_i\left(\vec{l},\vec{r},\mathbf{R}\right) = \left\|\vec{a_i} - \vec{r} - \mathbf{R}\vec{b_i}\right\|^2 - \|\vec{l_i}\|^2 = 0 \tag{5}$$

$$\Phi\left(\vec{l}\right) = \min \sum_{i=0}^{N-1} \psi_i \tag{6}$$

Where, $\psi_i$ is the length error function associated with the $i^{th}$ cable, which is used to minimize the function $\Phi$, representing the sum of all errors $\psi_i$. Therefore, the position and angle values that minimize the error will be the results of the forward kinematics problem and consequently, will be taken as the current values of the end-effector.

### D. Control System

When designing the exoskeleton control system, it should be considered that the D2W seeks to implement the *Assistance-As-Needed* (AAN) model. This model is characterized by combining the action of the exoskeleton with the patient's own activity during rehabilitation, in such a way as to provide the least amount of robotic assistance necessary for the correct performance of movements. Several studies have demonstrated the efficacy of AAN models, since they promote neuroplasticity, motor learning and reduce the duration and costs of therapies. [14], [15].

Exoskeletons following the AAN model must perform a constant adaptation to the patient's gait, basing their control on a reduction of the error made when performing movements [14].

Therefore, to implement the AAN model, a mechanical impedance control system is established. This is a type of controller used in robotics which takes into account the dynamic interactions that the system undergoes with the environment, resembling the movement of the robot to a spring-damper system. Unlike a position control, it does not seek to reach the target positions regardless of the forces applied to do so, but will take into account the dynamic interactions with the environment to moderate the forces applied without these being excessive. In other words, instead of following a rigid trajectory, there is a balance between reaching the target positions and maintaining a safe and stable interaction, which is fundamental in robot-human interfaces.

Based on the above and the exoskeleton architecture, the implemented control loop is shown in Fig. 6. In this loop, the torques applied on the motors are calculated by impedance control following (7):

$$F_i = K_S\xi_{l_i} + K_D\xi_v \tag{7}$$

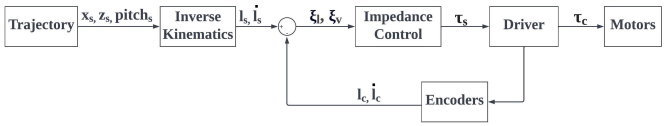


Fig. 6: Exoskeleton control loop based on mechanical impedance control. $\tau_s$ and $\tau_c$ represents the setpoint and actual torque applied to each motor; $l_s$ and $l_c$ are the setpoint and actual length of the cables; $\dot{l}_s$ and $\dot{l}_c$ are the setpoint and actual cable length variation rate ; $\xi_l$ and $\xi_v$ are the length and speed errors.

If we analyze (7), we observe that the calculated cable tension for the $ith$ cable $F_i$ is formed by two terms, a length error ($\xi_{l_i}$) and a velocity error ($\xi_{\dot{l}_i}$).

*The length error* ($\xi_l$) is obtained as the difference between the target length of the cables ($l_s$), which has been calculated by inverse kinematics; and the current length of the cables ($l_c$) measured by the encoders associated to the motors. Also, $\xi_l$ is multiplied by the stiffness coefficient ($K_S$), which will be varied according to the degree of assistance required by the patient. If the patient has very reduced mobility and requires greater robotic assistance (higher forces applied by cables), a higher value of $K_S$ is established.

*The velocity error* ($\xi_v$) is obtained as the difference between the target velocity of length variation of the cables ($\dot{l}_s$) and the real velocity ($\dot{l}_c$) measured by the encoders. This error is associated with the damping coefficient ($K_D$), which determines the rate and oscillation of the exoskeleton position variation.

For each iteration of the control loop, the tension force calculated by the mechanical impedance control is converted to torque setpoints and controlled on the motors to achieve the target positions.

## IV. Results

The technical evaluation of the system was performed by testing the system under a series of scenarios. These tests consisted of two stages: in the first, the end-effector movement was analyzed in a free-form manner without a patient using the insole following a gait-like trajectory, (Fig. 7a). In the second test, the exoskeleton controlled the motion of a healthy adult over the same trajectory (Fig. 7b). The aim was to analyze how the exoskeleton behaved when weight was exerted on the end-effector, and in the absence of weight.

In both tests, direct kinematics were used to measure the actual position of the end-effector in the *x* and *z* directions, as

well as its *pitch* rotation. Also, in order to compare the setpoint trajectories with the real ones, the mean absolute error (MAE) and the root mean square error (RMSE) were calculated for all measured values.

### A. Results on the Free End-Effector

To analyze the free motion of the end-effector (without a patient wearing the insole), the exoskeleton was subjected to 37 gait cycles following a fixed trajectory. Fig. 7a) shows a comparison between the mean of the trajectories measured during the 37 cycles (red function), versus the target trajectory (blue function). In addition, the MAE and RMSE of the measures are shown in Table I.

If we analyze the results obtained in the graphs for $x$ and $z$, we see that the trajectories performed by the exoskeleton are close to and follow the trend of the setpoints, which is verified in turn by the low position errors (RMSE and MAE) obtained with respect to the distance traveled during the movements. It is also observed that there is a certain time lag between the exoskeleton receiving a setpoint and reaching that position. This effect could be compensated by adjusting the parameters associated with the impedance control.

As for rotations, the exoskeleton presents greater difficulties in their execution. This is due to the absence of mass on the insole. By exerting the weight of the patient's leg on it, the insole will not have as much freedom of movement, resulting in less oscillatory trajectories and executing rotations with significantly greater precision.

### B. Results on the Test Subject

For these tests, the insole was worn by a healthy user to analyze whether the end-effector is able to correctly translate the movements to the test subject's ankle (Fig. 7b). In order to analyze the ability of the exoskeleton to guide movements, the subject tried to keep the leg as passive as possible, so that all the movement was originated by the robotic system.

The experiment consisted of performing 37 gait cycles following the same fixed trajectory as in the previous tests. Table II shows the MAE and RMSE calculated for the experiment.

TABLE I: RMSE and MAE Results on the Free End-Effector

| **Direction** | **Metrics** | |
|---|---|---|
| | ***RMSE*** | ***MAE*** |
| X (m) | 0.10 | 0.09 |
| Z (m) | 0.05 | 0.05 |
| Pitch (º) | 7.51 | 6.41 |

[a] Values of RMSE and MAE are in the same units as the direction.

TABLE II: RMSE and MAE Results on the Test Subject

| **Direction** | **Metrics** | |
|---|---|---|
| | ***RMSE*** | ***MAE*** |
| X (m) | 0.09 | 0.08 |
| Z (m) | 0.11 | 0.1 |
| Pitch (º) | 7.58 | 6.49 |

[a] Values of RMSE and MAE are in the same units as the direction.

The results obtained are graphically represented in Fig. 7b)

If we analyze the results obtained in the $x$ direction, these are still very accurate and there are no significant variations with respect to the experiment performed in the absence of the test subject, being its trajectory, MAE and RMSE practically identical. Therefore, the high effectiveness of the exoskeleton to perform longitudinal displacements in the walking direction is confirmed.

For the $z$ direction, analyzing the graphics, we found that it moves away from the setpoint positions. This is due to the fact that the increased weight on the insole opposes the vertical displacements. To improve these results, the torque exerted by the upper motors could be amplified, but it must be taken into account that these tests have been performed with an adult, so the leg of a child will have a much lower mass. Even so, the trajectory performed clearly follows the same pattern as the target.

Finally, as previously theorized, the ability to generate $pitch$ rotations improves with increasing weight on the insole. There is an obvious time lag when executing rotations. A possible solution is, during the closed control loop of the system (Fig. 6), instead of exercising impedance control over the cable length error, to exercise control over the position and rotation error of the end-effector, which will improve the precision of the movements.

It should also be remembered that the subject tries not to contribute to the leg movement, leaving the exoskeleton to do all the work. In a real case, the patient would also collaborate to reach the target trajectory, improving the results.

## V. Conclusions

After the tests performed, it can be concluded that in this study a new ankle control module has been developed and implemented with the capacity to act and guide the movement over three DOF, two translational ($x$ and $z$) and one rotational ($pitch$). At the same time, unwanted abduction-adduction rotations, are limited by the implemented mechanical structure, based on four motors mounted on double coil drums.

In addition, as its movement is regulated by a mechanical impedance control, the exoskeleton is able to implement the AAN model, in which the action of the robot is combined with the child's own activity.

On the other hand, the architecture of the exoskeleton is compatible with the D2W, allowing its easy incorporation into the overall system.

As for the future lines of the project, despite the positive results obtained during the experiments, for its complete clinical validation, it will be necessary to perform tests of its operation in children with CP, and compare these with the results of the current ankle control module of the D2W. In addition, in order to further improve its performance, the control loop of the exoskeleton could be modified so that the impedance control is performed on the end-effector position and rotation error, instead of on the cable length error.

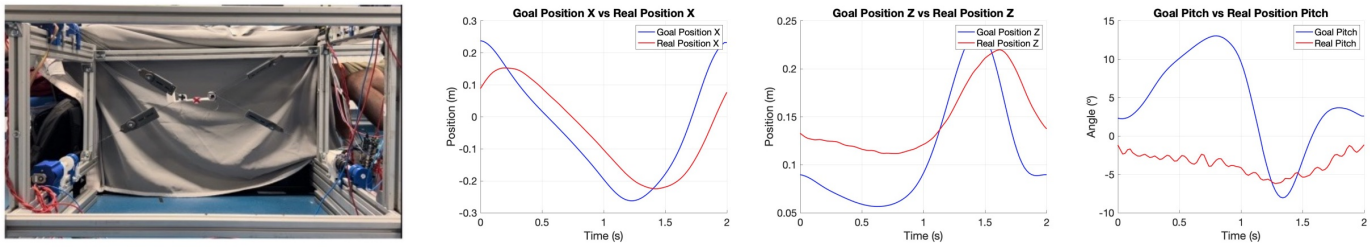


(a)

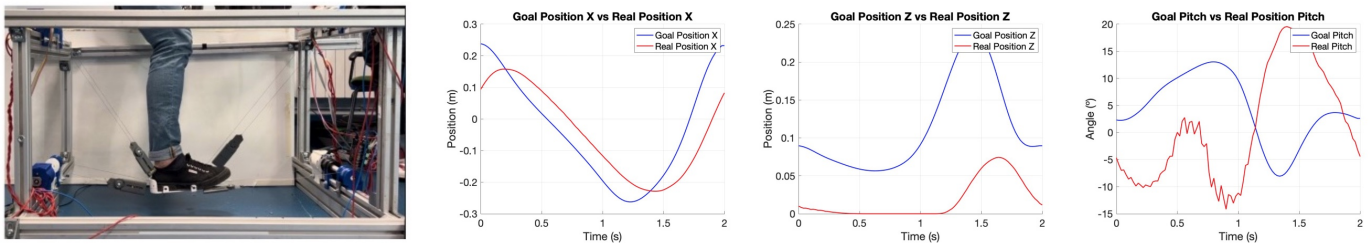


(b)

Fig. 7: Graphs of setpoint trajectory and actual trajectory performed by the end effector in: a) absence of test subject; b) the insole being used by a test subject.

## REFERENCES


[1] K. W. Krigger, "Cerebral palsy: an overview," Am. Fam. Physician, vol. 73, no. 1, pp. 91-100, Jan. 2006. [Online]. Available: https://www.ncbi.nlm.nih.gov/pubmed/16417071

[2] A. V. Patel, J. S. Hildebrand, C. R. Leach, P. T. Campbell, C. Doyle, K. Shuval, Y. Wang, and S. M. Gapstur, "Walking in relation to mortality in a large prospective cohort of older U.S. adults," Am. J. Prev. Med., vol. 54, no. 1, pp. 10-19, Jan. 2018. doi: 10.1016/j.amepre.2017.08.019.

[3] Z. F. Lerner, D. L. Damiano, H. S. Park, A. J. Gravunder, and T. C. Bulea, "A robotic exoskeleton for treatment of crouch gait in children with cerebral palsy: design and initial application," IEEE Trans. Neural Syst. Rehabil. Eng., vol. 25, no. 6, pp. 650-659, Jun. 2017. doi: 10.1109/TNSRE.2016.2595501.

[4] A. Meyer-Heim et al., "Improvement of walking abilities after robotic-assisted locomotion training in children with cerebral palsy," Arch. Dis. Child., vol. 94, pp. 615-620, Feb. 2009. doi: 10.1136/adc.2008.145458.

[5] H.I. Krebs, J.J. Palazzolo, L. Dipietro, M. Ferraro, J. Krol, K. Rannekleiv, B.T. Volpe, and N. Hogan, "Rehabilitation Robotics: Performance-Based Progressive Robot-Assisted Therapy," *Autonomous Robots*, vol. 15, no. 1, pp. 7-20, Jul. 2003. DOI: 10.1023/A:1024494031121.

[6] M. Zhang, T. C. Davies, y S. Xie, "Effectiveness of robot-assisted therapy on ankle rehabilitation–a systematic review," J. Neuroeng. Rehabil., vol. 10, p. 30, Mar. 21, 2013. doi: 10.1186/1743-0003-10-30

[7] S. Jezernik, G. Colombo, T. Keller, H. Frueh y M. Morari, "Robotic orthosis Lokomat: a rehabilitation and research tool," Neuromodulation, vol. 6, no. 2, pp. 108-115, 2003. doi: 10.1046/j.1525-1403.2003.03017.x.

[8] C. Schmidt-Lucke, J. Käferle, B.-M. Rydh Berner, L. Ahlborg, H. M. Hansen, U. Skjellvik Tollefsen, T. Thon, R. Damkjær Moen, A. Pekanovic, Å. B. Tornberg, and K. Lauruschkus, "Effect of assisted walking-movement in patients with genetic and acquired neuromuscular disorders with the motorised Innowalk device: an international case study meta-analysis," PeerJ, vol. 7, p. e7098, Jun. 2019. doi: 10.7717/peerj.7098.

[9] C. Bayón et al., "Development and evaluation of a novel robotic platform for gait rehabilitation in patients with Cerebral Palsy: CP-Walker," Robot. Auton. Syst., vol. 91, pp. 101-114, 2017. doi: 10.1016/j.robot.2016.12.015.

[10] C. M. Verónica Palomino-Díaz, P. Romero-Sorozábal, and G. Delgado-Oleas, "Diseño conceptual de una plataforma robótica para ayudar a que los niños con parálisis cerebral descubran cómo caminar," in XII Simposio CEA de Bioingeniería, 2021, pp. 83-88.

[11] S.H. Lee, G. Park, D.Y. Cho, et al., "Comparisons between end-effector and exoskeleton rehabilitation robots regarding upper extremity function among chronic stroke patients with moderate-to-severe upper limb impairment," *Sci Rep*, vol. 10, pp. 1806, 2020. doi: 10.1038/s41598-020-58630-2.

[12] P. Romero-Sorozabal, G. Delgado-Oleas, A. F. Laudanski, Á. Gutiérrez, and E. Rocon, "Discover2Walk: a cable-driven robotic platform to promote gait in pediatric population," IEEE/RSJ IROS., in press

[13] A. Pott, Cable-Driven Parallel Robots: Theory and Application, 1st ed., ser. Springer Tracts in Advanced Robotics. Springer, 2018. doi: 10.1007/978-3-319-76138-1.

[14] J. L. Emken, R. Benitez, and D. J. Reinkensmeyer, "Human-robot cooperative movement training: learning a novel sensory motor transformation during walking with robotic assistance-as-needed," J. Neuroeng. Rehabil., vol. 4, pp. 8, Mar. 2007.

[15] A. U. Pehlivan, D. P. Losey, and M. K. O'Malley, "Minimal Assist-as-Needed Controller for Upper Limb Robotic Rehabilitation," IEEE Trans. Robot., vol. 32, no. 1, pp. 113-124, Feb. 2016, doi: 10.1109/TRO.2015.2503726.

[16] A. Thevenon, F. Gabrielli, J. Lepvrier, A. Faupin, E. Allart, V. Tiffreau, and V. Wieczorek, "Collection of normative data for spatial and temporal gait parameters in a sample of French children aged between 6 and 12," Annals of Physical and Rehabilitation Medicine, vol. 58, no. 3, pp. 139-144, 2015. doi: 10.1016/j.rehab.2015.04.001.